Research Square

Preprints are preliminary reports that have not undergone peer review.
They should not be considered conclusive, used to inform clinical practice,
or referenced by the media as validated information.

Cerebellum–white-matter proportionality is associated with cognition but not explained by lobular anatomy

Baptiste Dumoulin

baptiste.dumoulin@chu-brugmann.be

CHU Brugmann University Hospital

Research Article

Keywords: Cerebellum, Cognition, Intelligence, Magnetic Resonance Imaging, Neuroimaging

Posted Date: November 19th, 2026

DOI: https://doi.org/10.21203/rs.3.rs-11566084/v1

License: This work is licensed under a Creative Commons Attribution 4.0 International License.
Read Full License

Additional Declarations: No competing interests reported.

Abstract

Background. A previously identified association between whole-cerebellum and cerebral-white-matter (Cer:WM) allocation and cognitive ability does not establish a lobular mechanism. We tested whether this association in Amsterdam Open MRI Collection (AOMIC) ID1000 was robust to a new cerebellar measurement and explained by regional allocation.

Methods. First-run T1-weighted scans from 928 participants were processed outcome-blind with FastSurfer/CerebNet v2.6.0. Before regional measurements were joined to cognition, the primary exposure was fixed as the log ratio of bilateral Crus I, Crus II and VIIb to bilateral lobules I-IV and V. Blinded quality control produced one anatomical exclusion; final analyses used 925 participants and adjusted for age, sex, tissue scale and five-part macroanatomical composition.

Results. The newly measured Cer:WM association remained positive (standardized β = 0.101, 95% CI 0.029–0.174, p=.0063; old/new cerebellar totals r=.982). The locked posterior:anterior ratio was null (β = 0.004, 95% CI -0.059-0.067, p=.908); its confidence interval excluded standardized effects of magnitude ≥ 0.067, and a post-hoc equivalence test supported equivalence within ± 0.10 (TOST p=.0014). The regional term attenuated the baseline macro Cer:WM coefficient by only 0.28%. Global lobular-composition and asymmetry tests were null, and regional augmentation was uninformative in cross-validation.

Conclusions. The AOMIC Cer:WM association is robust to cerebellar measurement method but is not explained by detectable lobular allocation in healthy young adults. Cerebral white matter and cerebellum showed markedly different intracranial-volume scaling (exponents 0.606 versus 0.372), underscoring allometric and compositional specification as an important benchmark for cerebellar morphometry.

Introduction

Total brain volume shows a modest positive association with intelligence, but overall size does not specify how tissue is distributed within brains of comparable size (Pietschnig et al. 2015). Brain compartments also scale non-isometrically with intracranial volume, so anatomical ratios and regional-volume coefficients can change meaning when different size models are used (de Jong et al. 2017).

In related macroanatomical work across HCP-YA, DLBS and AOMIC ID1000, a five-part compositional model separated analyzed-tissue scale from relative allocation among cortical gray matter, cerebral white matter, subcortical gray matter, cerebellum and brainstem using isometric log-ratio coordinates (Egozcue et al. 2003; Dumoulin 2026). That work identified a positive cerebellum:cerebral-white-matter (Cer:WM) balance in AOMIC ID1000. Pairwise balances are projections of a multivariate composition, however, and a positive Cer:WM coefficient does not by itself establish a specifically cerebellar mechanism.

A biologically plausible regional explanation is preferential allocation to posterior cerebellar association territories. Functional and connectivity studies consistently distinguish anterior sensorimotor territories from posterior cerebellar regions linked to association cortex (Stoodley and Schmahmann 2009; Buckner et al. 2011). CerebNet enables automated lobular segmentation from T1-weighted MRI with high test-retest reliability (Faber et al. 2022). In 932 Human Connectome Project participants, Lutz et al. (2025) reported numerous weak regional cerebellar–cognition associations after adjustment for age, sex and total brain volume.

Regional effects may also depend on developmental context. AOMIC ID1000 deliberately restricts age to 19–26 years (Snoek et al. 2021). Recent lifespan work shows heterogeneous cerebellar aging and posterior cerebellar associations with cognitive resilience (d'Oleire Uquillas et al. 2026), while developmental work demonstrates steeper growth of association territories and coordinated cerebello-cortical maturation (Manoli et al. 2026). A null cross-sectional regional-volume result in young adults would therefore define a boundary condition rather than exclude regional cerebellar contributions across the lifespan.

We therefore reprocessed the AOMIC ID1000 structural MRI cohort outcome-blind with FastSurfer/CerebNet. Before joining new regional measurements to cognition, we fixed one primary hypothesis: higher general cognitive ability would be associated with greater posterolateral association-cortex relative to anterior motor-cortex cerebellar volume beyond the complete macroanatomical composition. Secondary analyses tested measurement-method robustness of the macro association; explicitly post-hoc analyses examined broader lobular, predictive, compositional and allometric explanations.

Materials and methods

Participants and cognitive phenotype

AOMIC ID1000 is a community sample acquired on a Philips 3-T scanner and restricted to ages 19–26 years. The original study was approved by the University of Amsterdam faculty ethical committee (EC 2010-BC-1345), and participants provided informed consent after being informed about privacy and data sharing (Snoek et al. 2021). The present study is a secondary analysis of anonymized public data.

First-run structural T1 MRI was available for 928 participants. A pre-existing phenotype-complete analysis table contained 926 participants with age, sex, three Intelligence Structure Test (IST) domains and macroanatomical measures; all 926 matched the present CerebNet outputs. One participant was excluded after blinded targeted neuroradiology adjudication of the sole gross-screen-uncertain case, yielding N = 925 for final inference. General cognitive ability was the standardized first principal component of fluid, memory and crystallized IST domains defined before the present regional analyses. Native standardized IST total was retained for a contextual regional comparison. The final analysis sample is characterized in Table 1.

Relationship to related macroanatomical work

The macroanatomical baseline and cognitive outcome were defined before the present CerebNet analyses; their full specification is repeated here so the present study can be evaluated independently. The five positive tissue parts, in order, were cortical gray matter (C), cerebral white matter (W), subcortical gray matter (S), total cerebellum (Ce) and brainstem (B). With lX = ln(X), the four orthonormal Helmert isometric log-ratio coordinates were z1=(lC-lW)/sqrt(2), z2=(lC + lW-2lS)/sqrt(6), z3=(lC + lW+lS-3lCe)/sqrt(12), and z4=(lC + lW+lS + lCe-4lB)/sqrt(20); each coordinate was standardized within AOMIC. The baseline model contained centered age, sex, centered ln(C + W+S + Ce+B), and z1-z4. For targeted macro Cer:WM estimates, the same four-dimensional composition was orthogonally rotated so the first coordinate was ln(Ce/W)/sqrt(2), with the three orthogonal complements retained.

General cognitive ability was the first principal component of the population-SD-standardized fluid, memory and crystallized IST domains (weights 0.594, 0.564 and 0.574, respectively), oriented positively and re-standardized; this component explained 75.79% of the three-domain variance. These definitions reproduce those used in the related macroanatomical study (Dumoulin 2026), currently under review at Brain Structure and Function, which evaluates proportionality across HCP-YA, DLBS and AOMIC using pre-existing FreeSurfer summary measures. No CerebNet lobular analyses, regional QC, or the present regional, predictive or allometric analyses are reported in that manuscript.

Outcome-blind MRI processing and QC

First-run raw T1 images were processed with FastSurfer/CerebNet v2.6.0 using a fixed segmentation-only workflow (Henschel et al. 2020, 2022; Faber et al. 2022). Partial-volume-corrected Volume_mm3 values were retained. FastSurfer and CerebNet statistics were obtained for all 928 scans, and every scan contained all labels entering the locked primary contrast with positive finite values.

An outcome-blind 5-MAD screen across regional volumes, bilateral asymmetries and the locked ratio identified 10/928 scans for priority review; this was a review-priority device, not an automatic exclusion rule. A frozen minimum QC audit comprised all 10 priority scans plus 90 scans randomly sampled from the remaining cohort without cognitive outcomes. Mechanical verification required the anatomical reference, CerebNet segmentation and statistics; matching 256×256×256 geometry; valid transforms; positive finite statistics; all 27 encoded nonzero CerebNet labels; and exact agreement between segmentation voxel counts and .stats NVoxels. Standardized multi-plane overlays were used for outcome-blind gross screening of registration, cerebellar coverage and whole-cerebellum boundary failures.

All 90 random scans passed mechanical and gross screening. Among the 10 enriched priority scans, nine screen-passed and one was uncertain. The uncertain case was embedded among four comparison cases in a blinded mini-review by a neuroradiology reviewer who was not told which case had been flagged. The reviewer independently identified the same case as uncertain and, on focused follow-up,

recommended exclusion. Final outcome models were rerun after that imaging-based exclusion. Fine expert adjudication of every lobular boundary in all 100 screened cases was not performed. The outcome-blind analysis-lock and QC sequence are illustrated in Fig. 1.

[Insert Fig. 1 *here]*

Locked primary regional hypothesis

The primary exposure was the natural logarithm of bilateral Crus I + Crus II + VIIb volume divided by bilateral lobules I-IV + V volume. These non-overlapping labels were selected before new regional volumes were joined to cognition to contrast core posterolateral supramodal association territories with primary anterior sensorimotor territories. Lobule VI and lobule VIII were deliberately excluded from the locked ratio to sharpen this pole-to-pole contrast and avoid assigning transitional or secondary sensorimotor territories to either pole. The standardized exposure was added to the baseline model containing age, sex, log total analyzed-tissue volume and all four ILR coordinates of the five-part macroanatomical composition. HC3 robust confidence intervals and two-sided p-values were used. Missingness followed a complete-case policy.

Measurement-method robustness and sensitivities

To determine whether the macro association depended on the original FreeSurfer cerebellar estimate, the cerebellar component was replaced with a newly generated FastSurfer/CerebNet total defined as bilateral cerebellar cortical plus cerebellar white-matter volume. The five-part composition and focal Cer:WM balance were reconstructed under the same specification. This is a measurement-method robustness test within one cohort, not an independent-sample replication.

The locked regional model was repeated under alternative eTIV/size specifications, nonlinear allometry, education adjustment and predefined anatomical/influence sensitivities. Results were retained irrespective of direction or significance.

Post-hoc regional, predictive, compositional and allometric analyses

After the locked test was evaluated, all additional analyses were labeled post hoc. Twenty-five non-overlapping cerebellar cortical labels were represented as a 24-dimensional log-ratio composition and tested jointly. Ten bilateral left:right lobular ratios were tested jointly as an asymmetry block. Repeated 10-fold cross-validation compared the macroanatomical baseline with models additionally containing the locked ratio, all 24 lobular coordinates or the asymmetry block.

Coefficients from the four-dimensional five-part ILR regression were transformed back into a zero-sum log-contrast direction over the original tissue components and normalized to unit length. Participant

bootstrap resampling (2,000 iterations) quantified stability. Familiar pairwise balance vectors were compared with this multivariate direction by vector alignment.

Log-volume allometry to estimated intracranial volume (eTIV) was estimated separately for cortical gray matter, cerebral white matter, subcortical gray matter, the new CerebNet total cerebellum and brainstem with age and sex covariates. Tissue volumes residualized for age, sex and eTIV were then related to similarly residualized cognition separately and jointly. These models distinguish absolute-size relationships from fixed-total compositional allocation.

For contextual comparison with published HCP CerebNet work, a 32-feature AOMIC panel spanning bilateral lobules, vermis, cerebellar white matter, hemispheric cortical summaries and aggregate lobar measures was tested under age + sex + total-tissue adjustment. False-discovery-rate correction (Benjamini and Hochberg 1995) was applied across the feature family for each cognitive outcome. Because cohorts, acquisitions, regional definitions and cognitive instruments are not identical, this analysis is contextual rather than an exact replication.

AI-assisted research and manuscript preparation

OpenAI ChatGPT (accessed 27–30 October 2026) was used to assist with analysis planning, code drafting and debugging, workflow organization, QC triage, literature-search support, interpretation stress-testing and manuscript structure/language. Prompts asked the system to propose or critique analysis options, generate code from author-specified plans, summarize verifiable computational outputs and improve wording. All analyses were executed on source data with standard scientific Python libraries; the author inspected code and outputs, verified numerical results and references, made the final methodological and interpretive decisions, and takes responsibility for the submitted work. No generative-AI anatomical images were used.

Analysis-lock documents, executable analysis scripts and non-identifying aggregate output tables are supplied as Electronic Supplementary Material 2.

Table 1
Final AOMIC ID1000 analysis sample

Characteristic	Value
Final analysis N	925
Age, years	22.85 ± 1.71 (range 19–26)
Female / male	481 / 444
Education: low / medium / high	89 / 397 / 439
Estimated intracranial volume, mm^3	1,645,645 ± 214,034
Analyzed tissue volume, mm^3	1,220,307 ± 118,569
Original FreeSurfer total cerebellum, mm^3	150,323 ± 15,085
New FastSurfer/CerebNet total cerebellum, mm^3	130,646 ± 13,077
Posterior:anterior regional ratio	3.98 ± 0.43

Results

MRI yield, QC and measurement agreement

All 928 processed scans produced whole-brain and CerebNet statistics, and all 926 phenotype-complete participants matched the new measurements. The frozen gross-QC sample contained all 10 priority scans and 90 prespecified random scans. The random 90 had 0 gross failures and 0 uncertain cases; the enriched priority set had nine screen-passes and one uncertain case. Blinded targeted neuroradiology review independently identified that same case and recommended exclusion. Final inference therefore used N = 925. New and original total cerebellar volumes correlated r=.982; the new estimate was on average 13.1% smaller, confirming a meaningful change in measurement scale rather than numerical identity.

The macro Cer:WM association survives the new cerebellar measurement

Reconstructing the five-part composition with the new FastSurfer/CerebNet cerebellar total reproduced the focal AOMIC macro association: standardized Cer:WM β = 0.1014 (95% CI 0.0287–0.1741, p=.00630). The corresponding old-measurement estimate in the same final sample was β = 0.0988 (95% CI 0.0263–0.1713, p=.00761). Under eTIV-only adjustment, the new Cer:WM coefficient attenuated to β = 0.0248 (p=.494), whereas including eTIV alongside analyzed-tissue scale preserved the association (β = 0.1020, p=.00567).

The locked posterior:anterior hypothesis is unsupported

The prespecified posterolateral-association:anterior-motor ratio was essentially unrelated to general cognitive ability after full macrocomposition adjustment: β = 0.0037 (HC3 SE = 0.0320, 95% CI -0.0591 to 0.0666, p=.9078). The confidence interval was entirely contained within ± 0.067 standardized units. In a post-hoc precision analysis using symmetric equivalence bounds of ± 0.10 standardized units as a conventional small-effect benchmark, two one-sided tests supported equivalence (TOST p=.0014; residual df = 916). Added R2 was 0.000013 (0.0013 percentage points). Every locked sensitivity remained null. The baseline macro Cer:WM coefficient changed by only 0.28% after adding the regional measure. Fluid, memory and crystallized IST domains were also null for the locked ratio (all p≥.44). The principal standardized associations are summarized in Table 2 and visualized in Fig. 2.

[Insert Fig. 2 *here]*

Broader lobular information does not reveal a hidden volumetric signature

Adding the complete 24-dimensional lobular composition yielded HC3 Wald χ^2=21.32, df = 24, p=.620. A 10-dimensional bilateral asymmetry block was also null (χ^2=10.01, df = 10, p=.440), and no individual exploratory lobular component survived FDR correction. In the separate contextual native-IST-total regional screen, broader aggregate definitions that included lobule VI (SPL_VI-CrusI-CrusII-VIIb) or lobules VIII/IX (IPL_VIIIa-VIIIb-IX) were likewise null (p=.643 and p=.152, respectively; Table S8). Across 20 repeated 10-fold partitions, mean out-of-sample ΔR^2 relative to the macroanatomical baseline was − 0.0022 for the locked ratio, -0.0346 for the full lobular composition and − 0.0125 for the asymmetry block.

The multivariate composition points more strongly to cortical-gray versus cerebral-white allocation

Back-transformation of the five-part ILR association yielded unit log-contrast weights of + 0.621 for cortical gray matter, − 0.769 for cerebral white matter, + 0.080 for subcortical gray matter, + 0.117 for cerebellum and − 0.050 for brainstem. In 2,000 participant bootstraps, only the cortical-gray positive interval (+ 0.087 to + 0.800) and cerebral-white negative interval (− 0.858 to − 0.297) excluded zero. The cortical-gray:cerebral-WM pairwise balance aligned strongly with the multivariate direction (0.983), whereas Cer:WM showed moderate alignment (0.627). Repeating the transformation with the original cerebellar measure produced a nearly identical multivariate direction (cosine similarity = 0.9990). The back-transformed estimates and bootstrap intervals are displayed in Fig. 3.

[Insert Fig. 3 *here]*

Allometry separates relative allocation from absolute volume

The eTIV scaling exponent was 0.606 for cerebral white matter (95% CI 0.539–0.674), 0.488 for cortical gray matter (0.436–0.541) and 0.372 for new cerebellar volume (0.315–0.429). The cerebral-WM minus cerebellum exponent difference was 0.235 (95% bootstrap interval 0.171–0.301). After adjustment for age, sex and eTIV, residual cortical-gray (β = 0.187), subcortical-gray (β = 0.114), cerebellar (β = 0.092) and cerebral-WM (β = 0.082) volumes were each positively associated with g when tested separately. In a joint residual-volume model, cortical gray was the only clear unique association (β = 0.180, p = 5.2×10^{-6}); cerebral WM was not negatively associated (β=−0.030, p=.496). The negative cerebral-WM compositional weight therefore describes relative allocation under a fixed-total constraint, not evidence that lower absolute white-matter volume is beneficial.

Contextual regional comparison

Under the conventional regional model, no AOMIC CerebNet feature survived FDR correction for g, fluid, memory, crystallized ability or native IST total. For native IST total, the minimum unadjusted p was .112 and the minimum q was .799. Mean regional anatomy was highly concordant with published HCP CerebNet means (r=.9993 across 29 directly comparable summaries). Because HCP and AOMIC differ in acquisition, cognitive batteries and sample structure, this should not be framed as a formal failure to replicate Lutz et al. (2025); rather, broad regional volumetric associations were not readily recovered in a similarly sized independent young-adult dataset. Secondary and post-hoc findings are summarized in Table 3.

Table 2
Principal standardized associations

Model	N	β	95% CI	p
Macro Cer:WM, new measurement	925	0.101	0.029 to 0.174	.006
Locked posterior:anterior ratio, g	925	0.004	-0.059 to 0.067	.908
Locked ratio, fluid ability	925	0.009	-0.053 to 0.071	.771
Locked ratio, memory	925	-0.025	-0.091 to 0.041	.457
Locked ratio, crystallized ability	925	0.025	-0.038 to 0.087	.437
Note. HC3 robust inference; all p-values are two-sided.				

Table 3
Secondary and post-hoc analyses supporting interpretation

Analysis	Estimate	Inference / detail
24-df lobular-composition block	Wald χ^2=21.32	p=.620
10-df asymmetry block	Wald χ^2=10.01	p=.440
Cross-validation: locked ratio	mean ΔR^2=−0.0022	20 repeated 10-fold splits
Cross-validation: 24 lobular coordinates	mean ΔR^2=−0.0346	20 repeated 10-fold splits
Cortical-gray compositional weight	+ 0.621	bootstrap 95% interval + 0.087 to + 0.800
Cerebral-white compositional weight	−0.769	bootstrap 95% interval − 0.858 to − 0.297
Cerebral-WM eTIV exponent	0.606	95% CI 0.539–0.674
Cerebellum eTIV exponent	0.372	95% CI 0.315–0.429

Discussion

The present study separates a robust macroanatomical association from a specific regional explanation that was not supported. The AOMIC Cer:WM association persisted when the original cerebellar volume was replaced by a separately generated FastSurfer/CerebNet estimate. Yet preferential allocation to posterolateral association lobules-the most direct volumetric explanation fixed before outcome testing-was essentially unrelated to cognitive ability and did not attenuate the macro coefficient. The 95% confidence interval (-0.059 to 0.067) also places a tight precision bound on the null result; a post-hoc TOST supported equivalence within ± 0.10 standardized units, arguing against even a conventional small regional effect in this cohort.

The broader regional analyses reinforce that conclusion. Neither complete lobular composition nor asymmetry added explanatory or predictive value beyond the macroanatomical model. This does not imply that posterior cerebellar circuits are functionally irrelevant to cognition. Volume is a coarse phenotype; functional coupling, microstructure, developmental trajectory or disease-related reserve may show relationships that stable young-adult lobular volume does not capture.

This distinction is important in light of the literature. Lutz et al. (2025) reported numerous weak regional volume–cognition associations in HCP young adults. More recent lifespan work links posterior cerebellar integrity to cognitive resilience in aging (d'Oleire Uquillas et al. 2026), and developmental work identifies steeper growth of association territories and cerebello-cortical co-maturation (Manoli et al. 2026). AOMIC's deliberately narrow 19–26-year age range removes much age-related variance. The

present finding is therefore best interpreted as a boundary condition on cross-sectional regional volume in healthy young adulthood, not as a general rejection of regional cerebellar contributions to cognition.

The full compositional model further suggests that Cer:WM is not a uniquely cerebellar axis. Its outcome-associated direction was dominated by opposing cortical-gray and cerebral-white relative weights, whereas the cerebellar weight was smaller and its bootstrap interval included zero. The cortical-gray:cerebral-WM balance aligned much more strongly with this direction than Cer:WM. Thus the focal Cer:WM balance appears to be one projection of a broader tissue-allocation geometry.

Allometry clarifies why a negative cerebral-WM relative weight can coexist with a positive association of cerebral-WM residual volume with cognition. Cerebral white matter scaled substantially more steeply with intracranial size than cerebellum (eTIV exponents 0.606 versus 0.372), consistent with prior epidemiological MRI work (de Jong et al. 2017). This difference is directly relevant to cerebellar morphometry: linear adjustment against total tissue, white matter or intracranial size can change the interpretation of an apparent whole-cerebellum association when compartments scale non-isometrically. A fixed-total composition asks which tissue receives a larger share of a constrained whole, whereas eTIV-residual models ask whether a compartment is larger than expected for head size. These are different statistical and biological questions; the data provide no basis for claiming that less white matter is intrinsically advantageous.

The study also illustrates a broader methodological issue in morphometric cognition research. Highly correlated anatomical features can yield apparently specific regional coefficients while adding little or no out-of-sample information beyond global size and composition. Lewis et al. (2024) similarly showed that additional cortical morphometric measures did not reliably improve intelligence prediction beyond brain volume. Here, adding 24 cerebellar composition coordinates reduced cross-validated R^2, arguing against a strong stable volumetric lobular signature of g in this cohort.

Strengths

Strengths include outcome-blind reprocessing of 928 public structural scans, a regional hypothesis fixed before outcome linkage, same-cohort measurement-method robustness, explicit compositional modeling, complete reporting of a strong null result, allometric sensitivity and out-of-sample predictive checks. Technical processing yield was complete. A frozen 100-scan outcome-blind audit found no gross segmentation failures, and the sole uncertain case was independently identified in blinded targeted neuroradiology review and excluded before the final rerun without changing the conclusions.

Limitations

Limitations include the cross-sectional design; the fact that only the posterior/anterior test was locked prospectively with respect to the new regional outcomes; the narrow 19–26-year age range; differences between AOMIC and HCP in acquisition, cognitive instruments and sample structure; and the use of standardized gross QC rather than exhaustive expert fine-boundary adjudication of every lobule. Only the

sole screen-uncertain case underwent targeted expert review, so subtle segmentation inaccuracies may remain among screen-pass cases. Finally, regional volume may be less informative than functional, microstructural or longitudinal cerebello-cortical phenotypes.

Conclusion

In AOMIC ID1000, a macroanatomical cerebellum:cerebral-white-matter association with cognitive ability is robust to a newly generated cerebellar measurement but does not resolve into detectable posterior/anterior or broader lobular volumetric specialization. The broader association aligns more strongly with cortical-gray versus cerebral-white relative allocation and is sensitive to the model used to handle brain size. Because cerebral white matter and cerebellum scale differently with intracranial volume, allometric and compositional specification should be treated as a methodological benchmark when interpreting cerebellar morphometry-behavior associations. Future work should prioritize developmental, microstructural and functional organization rather than additional unstructured lobular searches.

Declarations

Acknowledgements: The author thanks the investigators and participants of the Amsterdam Open MRI Collection and the neuroradiology reviewer who performed blinded adjudication of the sole uncertain QC case.

Funding: No funds, grants, or other support were received for the submitted work.

Competing interests: The author has no relevant financial or non-financial interests to disclose.

Ethics approval: The original AOMIC ID1000 study was approved by the University of Amsterdam faculty ethical committee (EC 2010-BC-1345). The present work is a secondary analysis of anonymized publicly available data.

Consent to participate: Participants in the original ID1000 study provided informed consent and were informed about privacy and data sharing, as described by Snoek et al. (2021).

Consent to publish: Not applicable; no identifiable participant information is reported.

Data availability: AOMIC ID1000 raw and derivative data are publicly available through OpenNeuro (dataset ds003097). No raw MRI is redistributed with this manuscript.

Code availability: Analysis-lock documents, executable analysis scripts and non-identifying aggregate result tables are supplied with this submission as Electronic Supplementary Material 2.

Author contributions: Baptiste Dumoulin: Conceptualization, Methodology, Formal analysis, Investigation, Data curation, Visualization, Writing – original draft, Writing – review and editing.

AI use declaration: OpenAI ChatGPT (accessed 27–30 October 2026) assisted with analysis planning, code drafting/debugging, workflow organization, QC triage, literature-search support, interpretation stress-testing and manuscript structure/language. All analyses were run on verifiable source data; the author inspected code and outputs, verified numerical results and references, made the final methodological and interpretive decisions, and takes full responsibility. No generative-AI anatomical images were used.

References

1. Benjamini Y, Hochberg Y. Controlling the false discovery rate: a practical and powerful approach to multiple testing. J R Stat Soc Ser B Stat Methodol. 1995;57:289–300. https://doi.org/10.1111/j.2517-6161.1995.tb02031.x.
2. Buckner RL, Krienen FM, Castellanos A, Diaz JC, Yeo BTT. The organization of the human cerebellum estimated by intrinsic functional connectivity. J Neurophysiol. 2011;106:2322–45. https://doi.org/10.1152/jn.00339.2011.
3. de Jong LW, Vidal JS, Forsberg LE, et al. Allometric scaling of brain regions to intra-cranial volume: an epidemiological MRI study. Hum Brain Mapp. 2017;38:151–64. https://doi.org/10.1002/hbm.23351.
4. d'Oleire Uquillas F, Sefik E, Seidlitz J, et al. Cerebellar aging is spatially heterogeneous and supports cognitive resilience in later life. Nat Neurosci. 2026;29:1699–710. https://doi.org/10.1038/s41593-026-02289-x.
5. Dumoulin B. Brain Tissue Proportionality and General Cognitive Ability Across Three Adult Cohorts. Manuscript under review at Brain Structure and Function; 2026.
6. Egozcue JJ, Pawlowsky-Glahn V, Mateu-Figueras G, Barceló-Vidal C. Isometric logratio transformations for compositional data analysis. Math Geol. 2003;35:279–300. https://doi.org/10.1023/A:1023818214614.
7. Faber J, Kügler D, Bahrami E, et al. CerebNet: a fast and reliable deep-learning pipeline for detailed cerebellum sub-segmentation. NeuroImage. 2022;264:119703. https://doi.org/10.1016/j.neuroimage.2022.119703.
8. Henschel L, Conjeti S, Estrada S, Diers K, Fischl B, Reuter M. FastSurfer – a fast and accurate deep learning based neuroimaging pipeline. NeuroImage. 2020;219:117012. https://doi.org/10.1016/j.neuroimage.2020.117012.
9. Henschel L, Kügler D, Reuter M. FastSurferVINN: building resolution-independence into deep learning segmentation methods—a solution for high-resolution brain MRI. NeuroImage. 2022;251:118933. https://doi.org/10.1016/j.neuroimage.2022.118933.
10. Lewis JD, Imani V, Tohka J. Intelligence and cortical morphometry: caveats in brain-behavior associations. Brain Struct Funct. 2024;229:1417–32. https://doi.org/10.1007/s00429-024-02792-6.
11. Lutz G, Smerconish S, Roalf D, Neale MC, Schmitt JE. The genetics of cerebellar structure and associations with cognitive performance: a twin magnetic resonance imaging study. Hum Brain

Mapp. 2025;46:e70300. https://doi.org/10.1002/hbm.70300.

12. Manoli A, Magielse N, Hoffstaedter F, et al. Cerebellar growth is associated with domain-specific cerebral maturation and socio-linguistic behavior. Nat Commun. 2026;17:4338. https://doi.org/10.1038/s41467-026-72940-5.
13. Pietschnig J, Penke L, Wicherts JM, Zeiler M, Voracek M. Meta-analysis of associations between human brain volume and intelligence differences: how strong are they and what do they mean? Neurosci Biobehav Rev. 2015;57:411–32. https://doi.org/10.1016/j.neubiorev.2015.09.017.
14. van der Snoek L, van der Beemsterboer T, Eigenhuis A, Scholte HS. The Amsterdam Open MRI Collection, a set of multimodal MRI datasets for individual difference analyses. Sci Data. 2021;8:85. https://doi.org/10.1038/s41597-021-00870-6.
15. Stoodley CJ, Schmahmann JD. Functional topography in the human cerebellum: a meta-analysis of neuroimaging studies. NeuroImage. 2009;44:489–501. https://doi.org/10.1016/j.neuroimage.2008.08.039.

Figures

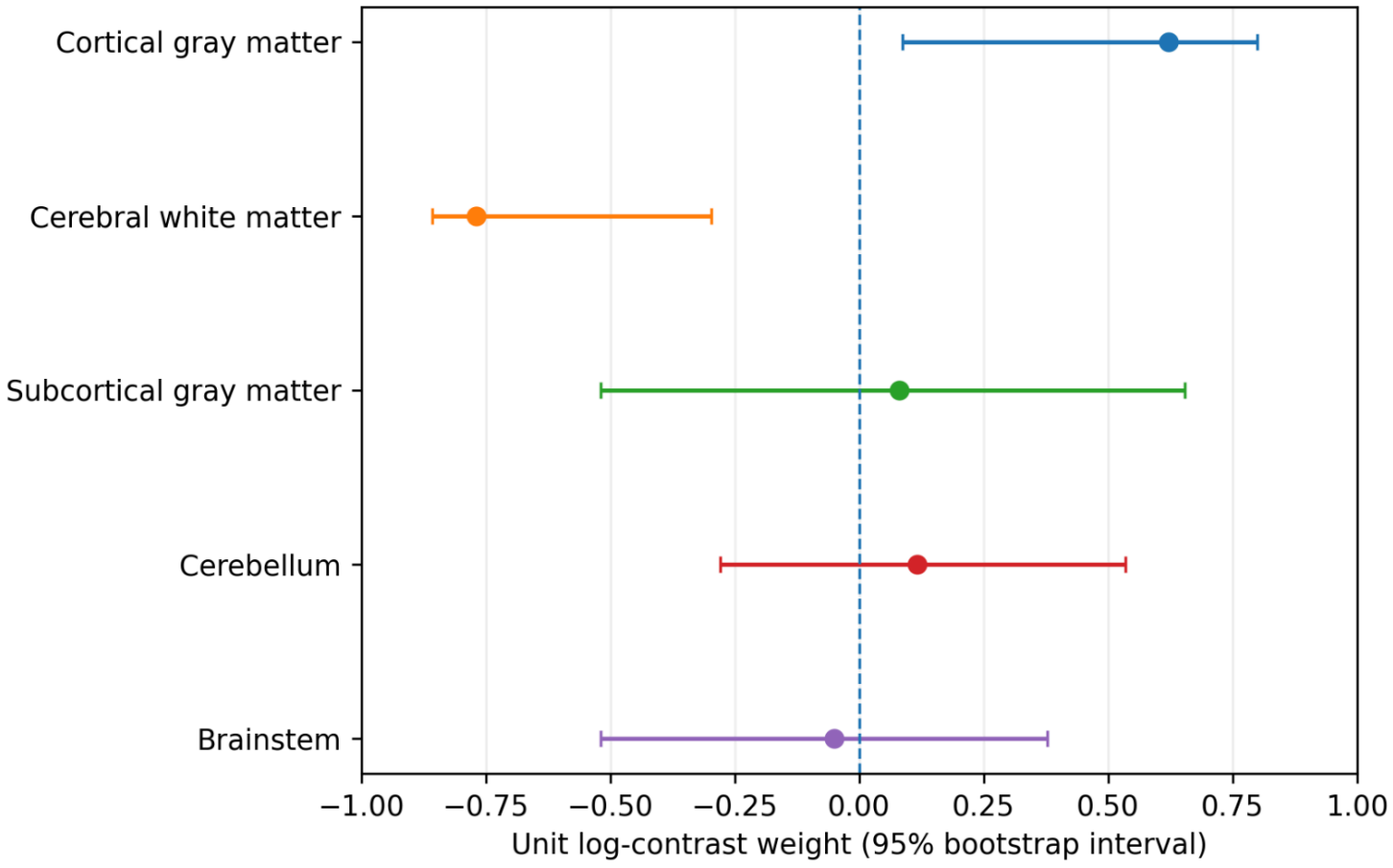

Figure 3

Back-transformed five-part compositional direction associated with general cognitive ability. Points are unit log-contrast weights; error bars are participant-bootstrap 95% intervals (2,000 resamples). Only cortical-gray and cerebral-white intervals exclude zero. Weights describe relative allocation and should not be interpreted as absolute-volume effects.

Supplementary Files

This is a list of supplementary files associated with this preprint. Click to download.

- 02ElectronicSupplementaryMaterial1v11.docx